

Scaling relations of supersonic turbulence in star-forming molecular clouds

Stanislav Boldyrev

Institute for Theoretical Physics, Santa Barbara, California 93106,
boldyrev@itp.ucsb.edu

Åke Nordlund

Copenhagen Astronomical Observatory and Theoretical Astrophysics Center, DK-2100
Copenhagen, Denmark,
aake@astro.ku.dk

Paolo Padoan

Harvard University, Department of Astronomy, 60 Garden street, Cambridge, MA 03138,
ppadoan@cfa.harvard.edu

ABSTRACT

We present a direct numerical and analytical study of driven supersonic MHD turbulence that is believed to govern the dynamics of star-forming molecular clouds. We describe statistical properties of the turbulence by measuring the velocity difference structure functions up to the fifth order. In particular, the velocity power spectrum in the inertial range is found to be close to $E_k \sim k^{-1.74}$, and the velocity difference scales as $\langle |\Delta u| \rangle \sim L^{0.42}$. The results agree well with the Kolmogorov–Burgers analytical model suggested for supersonic turbulence in [astro-ph/0108300]. We then generalize the model to more realistic, fractal structure of molecular clouds, and show that depending on the fractal dimension of a given molecular cloud, the theoretical value for the velocity spectrum spans the interval $[-1.74 \dots -1.89]$, while the corresponding window for the velocity difference scaling exponent is $[0.42 \dots 0.78]$.

Subject headings: MHD: Turbulence — ISM: dynamics — stars: formation

1. Introduction

Observations and numerical simulations of gas motion in molecular clouds show rather complex distributions of velocity and density fields, indicating that the motion is turbulent.

Although the nature and the scales of the driving force of the turbulence can vary, it has been established long ago that this turbulence is highly supersonic, with Mach numbers varying from cloud to cloud and reaching up to of the order of 30 at scales ~ 100 pc (Larson 1979, 1981, 1992; Falgarone & Phillips 1990; Falgarone, Puget, & Perault 1992; Myers & Gammie 1999; Padoan & Nordlund 1999, 2000; Ossenkopf & Mac Low 2000; Ostriker, Stone, & Gammie 2001).

Star formation is, of course, ultimately due to gravitational collapse of small Jeans-unstable cores. However, as is seen in high-resolution numerical simulation, the initial density fragmentation, that leads to creation of such cores, may be mainly due to strong supersonic turbulence, i.e. may be explained to large extent without invoking the effects of self-gravity (Padoan et al. 2001). The process of star formation can therefore be divided into two stages that may be approached separately. In the first stage, the supersonic, turbulent motion of the interstellar gas develops shocks that interact with each other and with the turbulent flow, which results in the emergence of rather complicated density structures. This stage should be described *statistically*, in terms of probability distribution of density and velocity fluctuations, or in terms of their moments; attempts to understand the complicated picture of turbulence by studying each particular structure can hardly be successful. On the other hand, the second stage, dealing with collapsing cores, can be approached on the grounds of classical dynamics, and depends on the effects of gravity and of the specific environment (e.g., pressure, temperature, magnetic fields). These two stages are not independent, however, since the first one sets the distribution of initial conditions for the second one, for further discussion see, e.g., Padoan & Nordlund (1999); Klein, Fisher, & McKee (2000); Burkert (2001); Klessen (2001); Elmegreen (2001). Even more, with some suitable definition of density clumps, the first stage of density fragmentation leads to the distribution of clumps over masses that already resembles the observed initial mass distribution function of stars (Padoan & Nordlund 2000; Padoan et al. 2000).

In this paper we address both numerically and analytically the first, “turbulent” stage of star-formation. So far, there has been no analytical theory predicting the statistical properties of supersonic interstellar turbulence, notwithstanding the fact that supersonic conditions have been inferred from observations for more than 20 years. In particular, the turbulence scaling relations, referred to as the Larson’s laws, concern the scaling of velocity and density fluctuations with respect to the size of the fluctuations (Larson 1979, 1981). These scalings seem to vary for different clouds, but most observations suggest that the velocity difference scaling scatters around $\langle |\Delta u|^2 \rangle^{1/2} \sim L^{0.4}$ (Falgarone, Puget, & Perault 1992). The corresponding velocity power spectra are steeper than the Kolmogorov one $E_k \sim k^{-5/3}$, which would correspond to $\langle |\Delta u|^2 \rangle^{1/2} \sim L^{1/3}$. As for the density fluctuations, the scaling of the peak density of fluctuations on scales L is close to $\rho(L) \sim L^{-1}$ (Falgarone,

Puget, & Perault 1992). However, these results should be taken with a certain degree of precaution. The error bars of available observations are rather large, and the systematic errors are sometimes unknown. Moreover, there are fundamental reasons that prevent one from restoring the three-dimensional velocity correlators from the measured two-dimensional projections (Ballesteros-Paredes & Mac Low 2001).

The high-resolution numerical results that recently became available (e.g. Padoan, Nordlund, & Jones 1997; Porter, Woodward, & Pouquet 1998; Mac Low 1999; Porter et al. 1999; Stone, Ostriker, & Gammie 1998; Padoan & Nordlund 1999, 2000; Padoan et al. 2000) shed some light onto the physics of supersonic turbulence. In this paper, we present numerical simulations of supersonic, super-Alfvénic turbulence, driven on large scales in such a way that the sonic Mach number M is of the order 10 and the Alfvénic Mach number M_a is of the order 3. An analysis of simulations with different Mach numbers will be presented elsewhere (Jimenez, Padoan & Nordlund 2001). We propose an analytical theory that explains the results of our numerical findings, and discuss its applicability to molecular clouds. We are interested mostly in the velocity correlators, although an application to the density statistics is presented as well. The next section analyzes the results of the numerical simulations. In particular, the velocity-difference structure functions are constructed. In section 3 we show that the observed features agree well with the recently proposed Kolmogorov–Burgers theory of supersonic turbulence. Section 4 discusses application of the results to molecular clouds. Conclusions are presented in section 5.

2. Scaling laws in numerical simulations of supersonic turbulence

The numerical simulations were performed with 250^3 and 500^3 resolutions for MHD turbulence with an isothermal equation of state, using the same method and program as in Padoan, Nordlund, & Jones (1997), Padoan & Nordlund (1999), Padoan et al. (2000), and Padoan et al. (2001). The turbulence was driven on large scales by a solenoidal external force with $1 \leq k \leq 2$, where $k = 1$ corresponds to the size of the periodic box. The solenoidal character of the forcing is not crucial for the velocity scaling in the inertial region—this was checked by comparing with runs with mixed compressional and solenoidal driving. The solenoidal driving was chosen to provide a better ‘boundary condition’ for the inertial interval in k space, since it turns out that the compressional to solenoidal ratio tends to become small in the inertial range. The external force sustains the supersonic gas motion ($M = 10$) in the simulations. The motions would otherwise decay on a time scale of the order of a crossing time and become sub-sonic due to the dissipation in shocks (Stone, Ostriker, & Gammie 1998; Padoan & Nordlund 1999). The real forcing is probably due to a turbulent

cascade from large scales, driven by supernovae and superbubbles (Korpi et al. 1999; de Avillez 2000),

The supersonic turbulence exhibits rather interesting properties that we summarize as follows. First of all, the spectra of both the potential, \mathbf{u}_c , and the solenoidal, \mathbf{u}_s , components of the velocity field are steeper than the Kolmogorov spectrum $k^{-5/3}$. These components are defined according to $\nabla \cdot \mathbf{u}_s = 0$ and $\nabla \times \mathbf{u}_c = 0$. In Fig. 1 we plot the solenoidal spectrum weighted by $k^{1.74}$, since the theory that we present below predicts for the velocity spectrum of turbulence $E_k \sim k^{-1.74}$. Second, the divergence-free, solenoidal part of the velocity field, \mathbf{u}_s , is generated quite effectively by such turbulence, contrary to the two-dimensional case, where turbulence without pressure is mostly potential. This effect of vorticity generation is analogous to the magnetic dynamo effect existing in 3D and non-existing in 2D turbulence (also, the presence of a magnetic field can help generate vorticity, as discussed by Vázquez-Semadeni, Passot, & Pouquet 1996). We find that the compressible part accounts for only 10–20 percent of the intensity of the velocity field, see Fig. 1. The ratio $\gamma = \langle u_c^2 \rangle / \langle u_s^2 \rangle$ can thus be chosen as a small parameter of the turbulence. Third, the dissipative structures look like two-dimensional shocks rather than one-dimensional filaments or vortices as in incompressible turbulence. To demonstrate this, we plot in Fig. 2 a randomly chosen two-dimensional cross-section of the density distribution in a physical simulation domain. The filaments seen on the picture correspond to the two-dimensional shock structures.

To quantitatively characterize the statistical properties of the turbulence we have measured the so-called structure functions of the velocity field (Frisch 1995). These functions are defined as:

$$S_p(L) = \langle |u(x+L) - u(x)|^p \rangle \sim L^{\zeta(p)}, \quad (1)$$

where u is the component of the velocity field perpendicular or parallel to the vector \mathbf{L} . According to the chosen component, the structure functions are called transversal or longitudinal, respectively. In the inertial interval, the structure functions obey scaling laws, and the exponents $\zeta(p)$ may be determined; it is usually expected that both transversal and longitudinal functions have the same scaling. The power spectrum of the velocity field is the Fourier transform of the second-order structure function, and may be expressed as $E_k \sim k^{-1-\zeta(2)}$.

We performed measurements of the structure functions up to $p = 5$. Since the Reynolds number in our simulations was not large enough to observe good scaling behavior of the structure functions, the method of Extended Self-Similarity (ESS) was applied. Namely, instead of plotting the structure functions themselves, we plotted the ratios of their logarithmic slopes. As was discovered by Benzi, et al. (1993) and Camussi & Benzi (1996), such ratios exhibit rather good (and correct) scaling behavior, even in systems with moderate

Reynolds numbers. Then, if one knows from the theory that the third order structure function scales with $\zeta(3) = 1$, or if any other scaling exponent $\zeta(n)$ is known from numerics or observations with good precision, one can obtain the scalings of all the other structure functions. To illustrate this procedure, in Fig. 3 we show the plots of the transversal structure functions, $S_1 \dots S_5$, their logarithmic slopes, and the ratios of the slopes vs that of S_3 . We chose to deal with the transversal rather than longitudinal functions since the flow is *shear-dominated*, and the transversal functions are therefore found to have a better scaling behavior. As illustrated by Fig. 3, the structure functions themselves do not exhibit good scaling behavior, but their relative scaling is well established in a rather large interval. As has been suggested by Dubrulle (1994), the ratios of scaling exponents may be universal while the scaling exponents themselves may be not. The reason is that the physical length L may not be a good scaling variable, and the universal scaling of all structure functions holds not with respect to L , but with respect to a certain function $\xi(L)$ that depends on the Reynolds number and other parameters of the system.

From Fig. 3 we conclude that the observed properties of the supersonic turbulence can hardly be predicted in the framework of any known model of strong turbulence. Indeed, the Kolmogorov model, or its generalizations to MHD, cannot be directly applied, since the turbulence has very small pressure and rather weak magnetic field. The model of turbulence without pressure, developed for the potential velocity field (the Burgers model), does not work either since the 3D turbulent flow generates vorticity. In the next section we present a theory of supersonic turbulence that explains the obtained spectra on the basis of the so-called She–Lévêque model of strong turbulence. This explanation was suggested in (Boldyrev 2001), and was motivated by recent successful application of the model to *incompressible* MHD turbulence (Biskamp & Müller 2000; Müller & Biskamp 2000).

3. Kolmogorov–Burgers model for supersonic turbulence

The analytical model hinges on the observation that in the inertial range the turbulence is mostly incompressible, obeying the Kolmogorov naive scaling laws of velocity fluctuations (see below), while in the dissipative range it behaves as Burgers turbulence, developing shock singularities. A model that relates the dissipative structures to the velocity scaling in the inertial interval was developed by She & Lévêque (1994) and She & Waymire (1995). As was pointed out by Dubrulle (1994), this model represents the velocity energy cascade as a log-Poisson process and can be obtained as a suitable limit of the so-called random β model of turbulence (see, e.g., Frisch 1995). In general, the She and Lévêque model has three input parameters. Two of them are the exponents of the naive (i.e. non-intermittent) scalings of

the velocity fluctuation, $u_l \sim l^\Theta$, and of the characteristic time of the energy transfer at this scale, $t_l \sim l/u_l \sim l^\Delta$. In our case these parameters are related, $\Delta = 1 - \Theta$, although in general this does not need to be so, as e.g. in the Iroshnikov-Kraichnan model of incompressible MHD turbulence (Grauer, Krug, & Marliani 1994; Politano & Pouquet 1995). The other parameter is the dimension of the most singular dissipative structure, D . The She–Lévêque formula, as generalized by Dubrulle (1994), then reads:

$$\zeta(p)/\zeta(3) = \Theta(1 - \Delta)p + (3 - D)(1 - \Sigma^{\Theta p}), \quad (2)$$

where $\Sigma = 1 - \Delta/(3 - D)$. Since in our case the velocity field in the inertial interval is mostly incompressible, one can imagine that the energy transfer is due to the Kolmogorov cascade, i.e., $\Theta = 1/3$, $\Delta = 1 - \Theta = 2/3$, while the dissipative structures are shocks, not filaments, so $D = 2$. With such input parameters, the formula gives:

$$\zeta(p)/\zeta(3) = \frac{p}{9} + 1 - \left(\frac{1}{3}\right)^{p/3}, \quad (3)$$

For the first five structure functions the model gives: $\zeta(1)/\zeta(3) = 0.42$, $\zeta(2)/\zeta(3) = 0.74$, $\zeta(4)/\zeta(3) = 1.21$, $\zeta(5)/\zeta(3) = 1.40$, in excellent agreement with the numerical results (cf. Fig. 3). To find the absolute scalings, we need to know the scaling of at least one of the structure functions. As we mentioned in Sec. 2, the Reynolds number is not large enough to see good scaling of the structure functions. However, it is known that the Fourier transform of the second order structure function, i.e., the velocity spectrum, can have larger scaling interval than the second order structure function itself. Thus, knowing from the measurement of the spectrum that $\zeta(2) \simeq 0.7 \cdots 0.8$, we infer $\zeta(3) \simeq 0.95 \cdots 1.08$, and the Kolmogorov relation, $\zeta(3) = 1$, may indeed hold in the inertial interval.

Note that our formula (3) coincides with the formula derived in (Biskamp & Müller 2000; Müller & Biskamp 2000) for incompressible MHD turbulence, where $\zeta(3) = 1$, and in this sense both systems belong to the same *class of universality*, in accord with the ideas put forward by Dubrulle (1994) and She & Waymire (1995). However, these two systems are completely different, and the Kolmogorov relation, $\zeta(3) = 1$, that is exactly proved in MHD, is *not* rigorously established in our case, but rather inferred from the numerical simulations. Strictly speaking, the scaling exponents can be different for these systems; it is their ratios that are reliably obtained from our numerical simulations and are believed to be universal. For instance, there is a possibility that these exponents can vary from cloud to cloud, depending on the equation of state, mechanisms of dissipation, Mach numbers, etc.

For completeness, we would like to present here a cartoon model which leads to the She–Lévêque formula. Our discussion is rather similar to the work of Dubrulle (1994). The reader not interested in the details of the derivation can safely skip to Sec 4. We start with

the simple β model of turbulence, formulated in a way suitable for generalization of the results to the random β model (a detailed discussion of such models may be found in (Frisch 1995)). Let us assume that our system is divided into boxes of size l and let us concentrate on the density of the velocity energy flux over scales in each box, ϵ_l . Now let us divide each box into smaller boxes, with size $l\Gamma$, where $\Gamma < 1$. The number of boxes increases, but now we want to leave only a fraction β of all newly formed boxes, and since the energy flux is constant, $\langle \epsilon_l \rangle = \text{const}$, the density of the energy flux in each box should be increased by $1/\beta$. After that, start decreasing the size of boxes again and repeat all the procedure exactly as in the previous step. One may introduce $W = \epsilon_{i+1}/\epsilon_i$, which takes the value $1/\beta$ with probability β , and 0 with probability $1 - \beta$ at each step, independently of previous steps. The fraction of space occupied by boxes decreases at each step, and one can easily check that eventually our boxes will cover the structure with fractal dimension

$$D = 3 - \log(\beta)/\log(\Gamma). \quad (4)$$

This is the dimension of the structure to which the cascade converges. It is easy to see that $\langle \epsilon_l^p \rangle \sim l^{\tau(p)}$, where

$$\tau(p) = \log\langle W^p \rangle / \log \Gamma. \quad (5)$$

Let us now apply this model to incompressible turbulence. According to the Kolmogorov refined similarity hypothesis, ϵ_l scales as u_l^3/l ; we will denote this as $\epsilon_l \approx u_l^3/l$. So we have

$$\zeta(p) = p/3 + \tau(p/3) = p/3 + (3 - D)(1 - p/3), \quad (6)$$

which gives, e.g., a velocity spectrum steeper than the Kolmogorov one. The β model produces the *linear* relation (6) which is not what is observed.

We now generalize this model in the following way. First, let us assume that the steps of size changes are very small, i.e., $\Gamma = 1 - x/(3 - D)$, and $\beta = 1 - x$, where $x \rightarrow 0$. These expressions are chosen to satisfy (4) up to the first order in small x . To modify the previous model we now assume that we do not disregard any newly formed boxes, whose fraction would be $1 - \beta = x$, but instead fill them with $W = \beta_1$, while the other boxes are filled with some factor $W = \beta_2$. This procedure leads to a so-called random β model. Since we have to preserve $\langle \epsilon_l \rangle = \text{const}$, we have to impose the relation $x\beta_1 + \beta_2(1 - x) = 1$ which gives $\beta_2 = 1 + x(1 - \beta_1)$. Using formula (5), we now derive $\tau(p) = C(\beta_1 - 1)p + C(1 - \beta_1^p)$, where we introduced the co-dimension $C = 3 - D$. If we now assume the Kolmogorov relation $\epsilon_l \approx u_l^3/l$, we immediately recover formula (2), where $\zeta(3) = 1$ and β_1 plays the role of Σ . This shows that Σ describes the degree of intermittency in the She–Lévêque model. However, in the compressible case the Kolmogorov relation is not proven. We can, however, hope that if we change the length variable $l \rightarrow \tilde{l} = \xi(l)$ in such a way that the

scaling exponent of the third-order structure function with respect to \tilde{l} becomes $\tilde{\zeta}(3) = 1$, the scaling of all the other structure functions will be restored as well. To achieve that we have to define the new scaling variable as $\tilde{l} = \xi(l) = \langle u_l^3 \rangle / \langle \epsilon_l \rangle$. Also, instead of the Kolmogorov relation, we assume $\epsilon_l / \langle \epsilon \rangle \propto u_l^3 / \langle u_l^3 \rangle$, which is suggested by the quadratic nonlinearity of the Navier-Stokes equation. Redefining the scaling $\tau(p)$ as $\langle \epsilon_l^p \rangle \sim \tilde{l}^{\tau(p)}$, we now easily get:

$$\zeta(p)/\zeta(3) = p/3 - C(1 - \beta_1)p/3 + C(1 - \beta_1^{p/3}), \quad (7)$$

which is the required generalization of the She-L ev eque formula. The unknown parameters β_1 and C can be obtained, e.g., from numerical simulations. In this formula it is not obvious that C is a co-dimension of the most singular dissipative structure, since the cascade was organized not with respect to physical length l , but with respect to \tilde{l} .

4. Application to molecular clouds

We now ask how adequate our numerical and analytical results are to real molecular clouds. The density structures of molecular clouds, as obtained from observations, are rather complicated, and one may question the validity of our simple model assuming shock singularities. In fact, observational relation of molecular cloud mass to the cloud size is close to $M \sim L^D$, where D is estimated to be greater than 2 see, e.g. Larson (1992), and also Elmegreen & Falgarone (1996), where the estimate $D = 2.3 \pm 0.3$ was presented. If the density were concentrated in elongated shocks, the scaling power would be 2. A plausible resolution lies in the assumption that over a range of scales (not available in numerical simulations due to limited resolution) dense structures are folded to form a complex distribution having *fractal* dimension $D \geq 2$; a complicated fractal (even multifractal) density distribution is indeed inferred from observations (Chappell & Scalo 2001). It seems natural to assume that the energy dissipation occurs mostly in shocks (Stone, Ostriker, & Gammie 1998; Ostriker, Stone, & Gammie 2001), and therefore the dissipative singularities should have the same dimension. Formula (2) thus relates the fractal dimension of a given molecular cloud to scaling properties of the velocity field in this cloud. In principle, this dimension can be different for different clouds, depending on mechanisms of cooling, dissipation, structure of magnetic fields, etc. Substitution of the fiducial value $D = 2.3$ in our formula (2) leads to even better agreement of the theory with recent observations, see Brunt & Heyer (2001), producing $\langle |\Delta u| \rangle \sim L^{0.55}$ and $E_k \sim k^{-1.83}$, where we assumed that the Kolmogorov relation $\zeta(3) = 1$ holds.

It is interesting to note that formula (2) also gives the upper boundary for the dimension of density distribution. The parameter Σ introduced in (2) measures the degree of intermittency of turbulence. For example, for $\Sigma \rightarrow 1$ one recovers the Kolmogorov, non-intermittent,

scaling $\zeta(p) = p/3$. By its definition, $0 \leq \Sigma \leq 1$, and therefore, $D \leq 2\frac{1}{3}$. Taking into account that on small scales the dissipative structures take the form of two-dimensional shocks, one may argue that the lower boundary for the density dimension is $D = 2$. We thus established a rather narrow window for D consistent with our theory. With the aid of formula (2) one then finds the corresponding intervals for the structure functions scaling exponents that are admissible in our theory. In particular, the first order exponent is expected to lie in the interval $[0.42 \cdots 0.78]$, and the second order exponent, related to the velocity spectrum, within $[0.74 \cdots 0.89]$. It is interesting that the observed value, $D = 2.3$, is rather close to the upper boundary. In Figs. 4 and 5 we plotted the scaling exponents $\zeta(1)$ and $\zeta(2)$ as functions of D for $2 \leq D \leq 2\frac{1}{3}$. We see that the exponents are very sensitive to the value of D , and it is therefore very hard to infer ζ 's from measurements of D – this would require measuring D with high precision. More practical test of the theory would be plotting observed $\zeta(2)$ versus $\zeta(1)$, our theory predicts that the values should lie on the line shown in Fig. 6.

5. Conclusions

The presented model proves to be rather successful in explaining the statistical properties of supersonic turbulence. In particular, we were able to explain the observational scaling relations of the turbulence in molecular clouds. It would be highly desirable to obtain a clear physical picture underlying the Log-Poisson energy cascade assumed in the derivation of (2). Also, the relation of the density distribution to the statistics of the velocity field requires a better understanding. Such a relation may be derived analytically in a simplified one-dimensional case (Boldyrev 1998; Boldyrev & Brandenburg 2001), although in the three-dimensional case the question is still open. However, in the derivation of formula (7) we explicitly constructed the *multifractal* distribution of the energy dissipation ϵ , which can possibly be related to the multifractal distribution of the density, since the energy dissipates in shocks where the density is accumulated. And finally, in the present paper we did not try to address the problem of the initial mass distribution of stars (but see Padoan & Nordlund 2000). The process of turbulent density fragmentation leads to creation of complicated density structures and sets the *initial conditions* for gravitationally unstable density clumps. The effects of self-gravity, and the dynamics of collapsing density cores fall beyond the scope of the present paper. All these are the questions for the future.

REFERENCES

de Avillez, M. A. (2000) MNRAS**315** 479.

- Ballesteros-Paredes, J. and Mac Low, M.-M. (2001), astro-ph/0108136.
- Benzi, R., Ciliberto, S., Tripicciono, R., Baudet, C., Massaioli, F., and Succi, S. (1993) Phys. Rev. E **48** R29.
- Biskamp, D. and Müller, W.-C., (2000) Phys. Plasmas **7** 4889.
- Boldyrev, S. (2001) astro-ph/0108300.
- Boldyrev, S., Phys. Plasmas, **5** (1998) 1681.
- Boldyrev, S. and Brandenburg, A., (2001) in preparation.
- Brunt, C. M. and Heyer, H. H., astro-ph/0110155.
- Burkert A., (2001) astro-ph/0105298.
- Camussi, R. and Benzi, R., (1996) Phys. Fluids Letters **9** 257.
- Chappell, D. and Scalo, J., ApJ **551** (2001) 712.
- Dubrulle, B., Phys. Rev. Lett. **73** (1994) 959.
- Elmegreen, B. G. (2001), in “From Darkness to Light”, ed. T. Montmerle & P. Andre, ASP Conference Series, in press; astro-ph/0010582.
- Elmegreen, B. G. and Falgarone, E., (1996), ApJ **471** 816.
- Falgarone, E. and Phillips, T. G., (1990) ApJ **359** 344.
- Falgarone, E., Puget, J.-L., & Perault, M. (1992) ApJ **257** 715.
- Frisch, U. (1995) *Turbulence* (Cambridge University Press).
- Grauer, R., Krug, J., and Marliani, C., Phys. Lett. A **195** (1994) 335.
- Jimenez, R., Padoan, P. and Nordlund, Å. (2001) in preparation.
- Klein, R. I., Fisher, R., and McKee, C. F., (2000) astro-ph/0007332.
- Klessen, R. S., ApJ (2001) to appear; astro-ph/0104127.
- Korpi, M. J., Brandenburg, A., Shukurov, A., Tuominen, I., & Nordlund, Å. (1999) ApJ **514** L99.

- Mac Low, M.-M., (1999), in *Interstellar Turbulence*, ed. J. Franco and A. Caramiñana, (Cambridge Univ. Press).
- Larson, R. B., MNRAS **186** (1979) 479.
- Larson, R. B., MNRAS **194** (1981) 809.
- Larson, R. B., MNRAS **256** (1992) 641.
- Müller, W.-C. and Biskamp, D., Phys. Rev. Lett. **84** (2000) 475.
- Myers, P. C. and Gammie, C. F., (1999), ApJ **522**, L141.
- Ossenkopf, V. and Mac Low, M.-M., (2000) astro-ph/0012247.
- Ostriker, E. C., Stone, J. M., and Gammie, C. F., (2001) ApJ **546**, 980; astro-ph/0008454.
- Padoan, P., Nordlund, A., & Jones, B. J. T. (1997) MNRAS **288** 145.
- Padoan, P. and Nordlund, Å., ApJ **526** (1999) 279.
- Padoan, P., Nordlund, Å., Rögnvaldsson, Ö. E., and Goodman, A. (2000) astro-ph/0011229.
- Padoan, P. and Nordlund, Å., (2000) astro-ph/0011465.
- Padoan, P., Juvela, M., Goodman, A. A., and Nordlund, Å. (2001) ApJ **553** 227.
- Politano, H. and Pouquet, A., Phys. Rev. E **52** (1995) 636.
- Porter, D., Pouquet, A., Sytine, I., and Woodward, P., Physics A **263** (1999) 263.
- Porter, D. H., Woodward, P. R., and Pouquet, A., Phys. Fluids **10** (1998) 237.
- She, Z.-S. and Lévêque, E., Phys. Rev. Lett. **72** (1994) 336.
- She, Z.-S. and Waymire, E. C., Phys. Rev. Lett. **74** (1995) 262.
- Stone, J. M., Ostriker, E. C., and Gammie, C. F., (1998) ApJ **508** L99.
- Vázquez-Semadeni, E., Passot, T., and Pouquet, A., ApJ **473** (1996) 881.

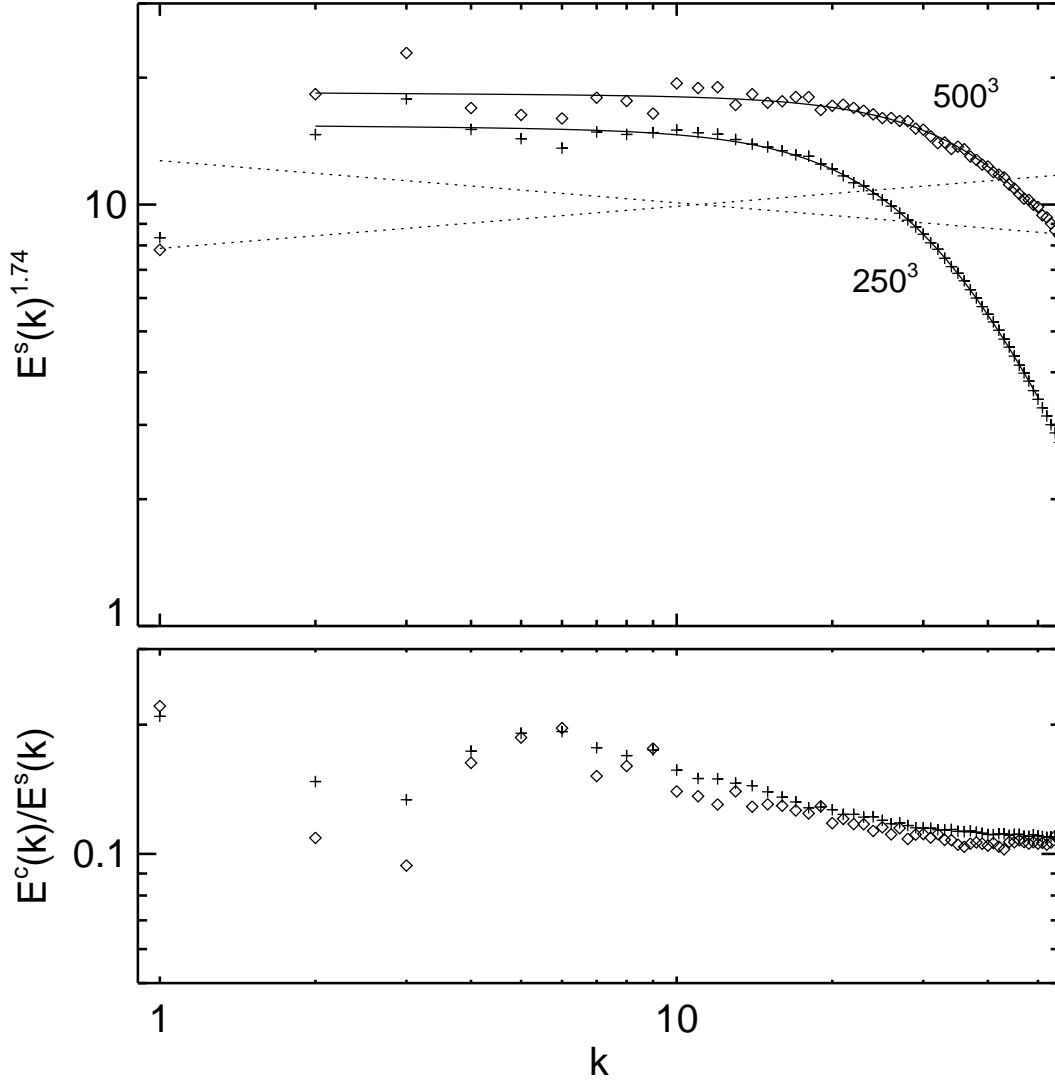


Fig. 1.— Power spectra of driven, super-sonic turbulence. The top panel shows the solenoidal power, compensated by $k^{1.74}$, and averaged over two turn-over times, after about three t.o. times from the start of the run, in a numerical experiment with resolution 250^3 (plusses), using random driving at $1 \leq k \leq 2$. Additional data points (diamonds) are from a 500^3 experiment, continued for about two tenths of a turn-over time from a 250^3 snapshot, which is enough to establish the extended large k solenoidal spectrum. The solid lines are least squares fits of the data in the range $2 \leq k \leq 50$ to functional forms $a/(k^p + bk^q)$, where p is the power law index in the inertial range (1.75 for the 250^3 case and 1.74 for the 500^3 case). Dashed lines show comparison slopes with spectral indices different by ± 0.1 , from 1.74. The bottom panel shows the average ratio of compressional to solenoidal power in the same experiments.

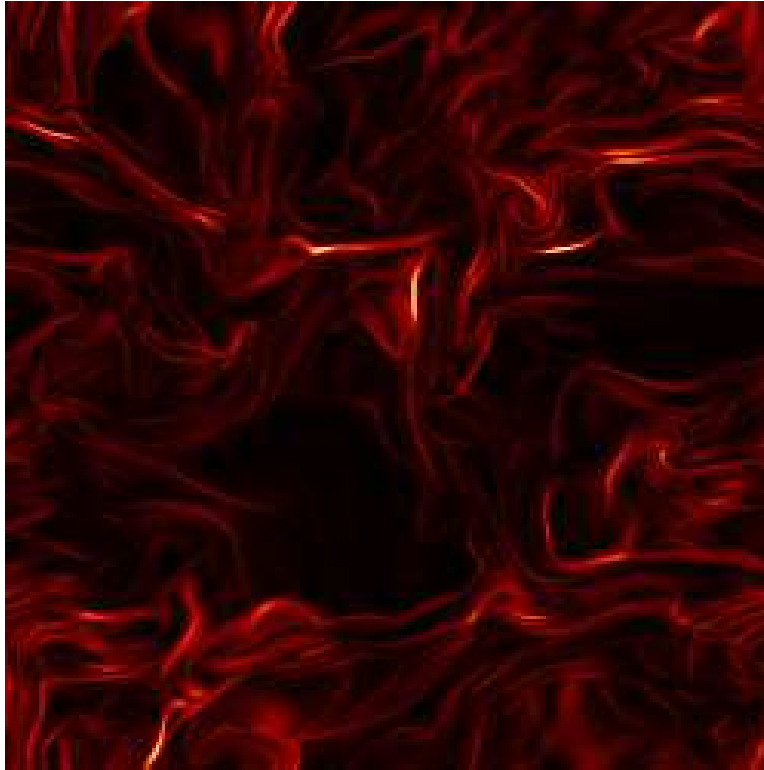


Fig. 2.— A random, two-dimensional cut through the physical simulation domain of a snapshot from a 250^3 experiment. The cross-section of the density field shows filamentary structures that correspond to sheet-like shock density structures.

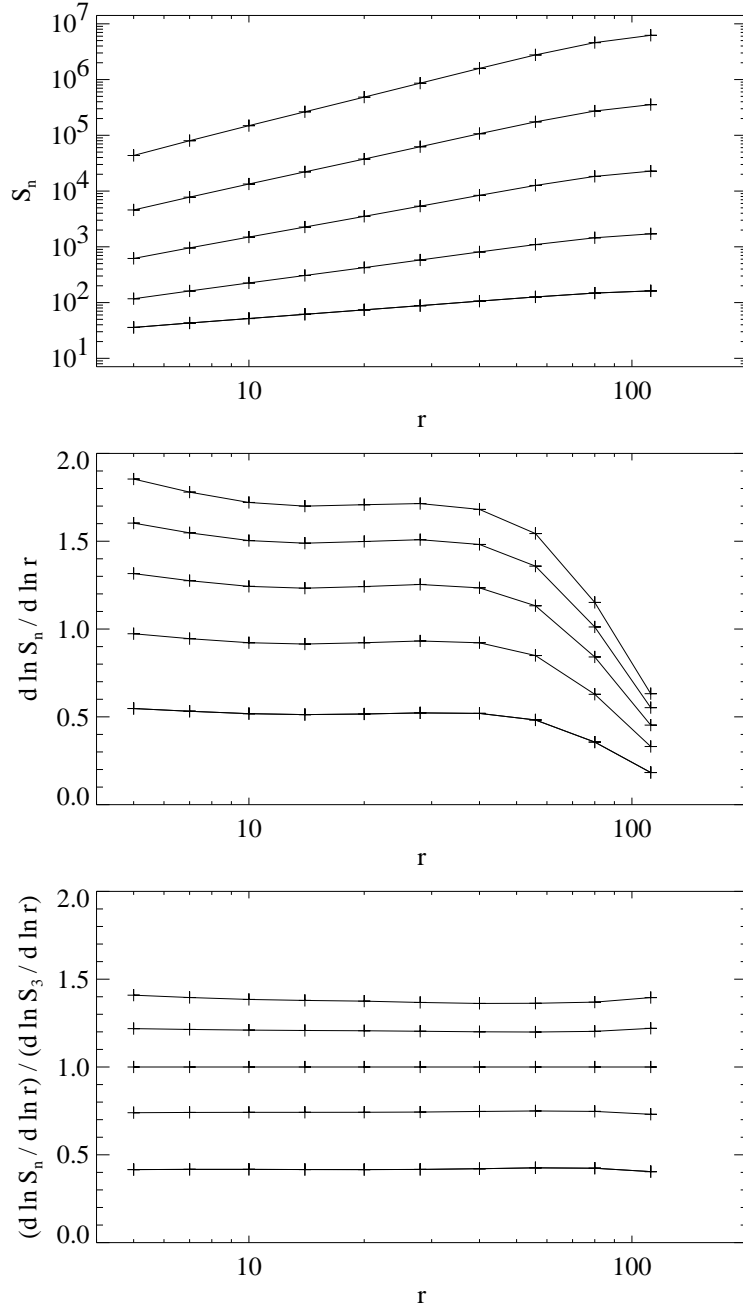


Fig. 3.— Transversal structure functions computed for $p = 1, 2, 3, 4, 5$ (correspondingly, from bottom to top in each panel). The first panel shows Log-Log plots of the structure functions. The second panel shows the differential slopes, $\zeta(1), \dots, \zeta(5)$. The scaling range is very short, due to the limited Reynolds number. The third panel presents the ratios of the differential slopes to $\zeta(3)$, which exhibit excellent scalings, in agreement with the Extended Self-Similarity hypothesis. These ratios are well described by our formula (3).

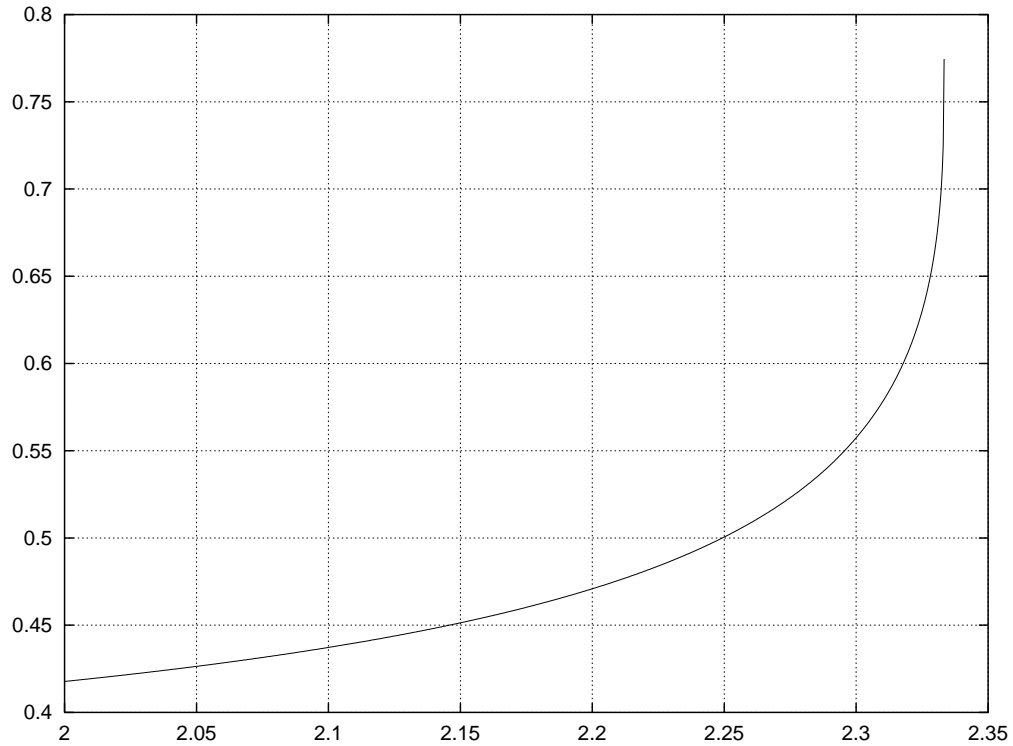


Fig. 4.— Normalized scaling exponent of the first-order structure function, $\zeta(1)/\zeta(3)$, as a function of the dimensionality, D , of the most singular dissipative structure, which can be close to the fractal dimensionality of the cloud. We use formula (2) with $\Theta = 1/3$, $\Delta = 2/3$ and D changes from 2 to $2\frac{1}{3}$. The results of our numerical simulations correspond to $D = 2$.

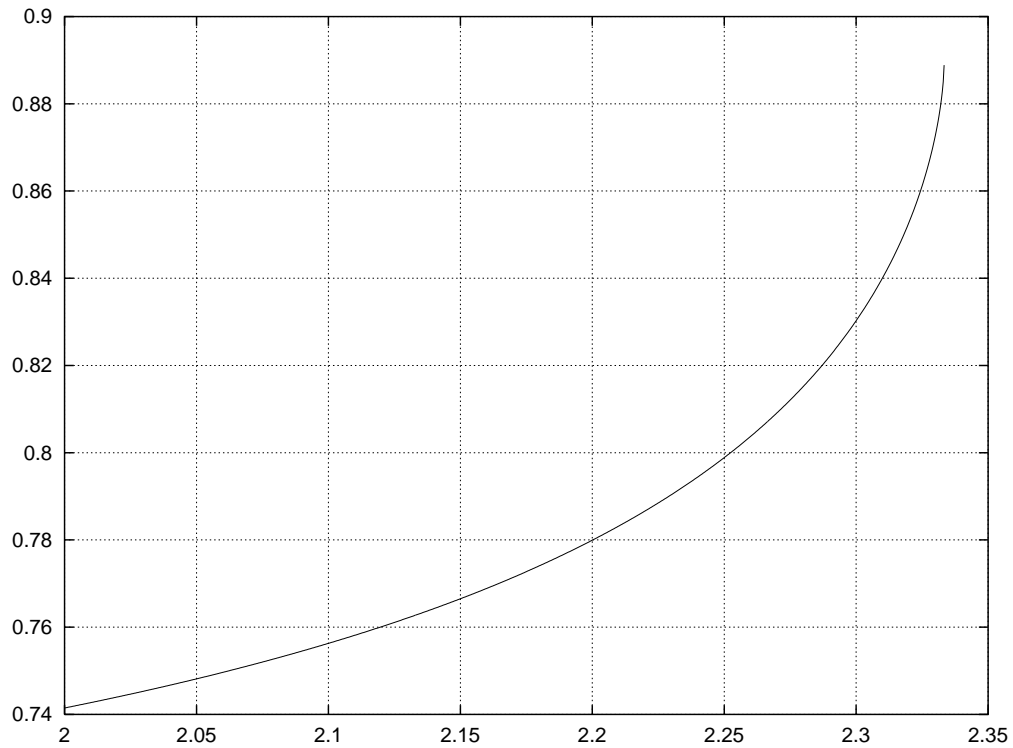


Fig. 5.— Normalized scaling exponent of the second-order structure function, $\zeta(2)/\zeta(3)$, as a function of the dimensionality, D , of the most singular dissipative structure, which can be close to the fractal dimensionality of the cloud. We use formula (2) with $\Theta = 1/3$, $\Delta = 2/3$ and D changes from 2 to $2\frac{1}{3}$. The results of our numerical simulations correspond to $D = 2$.

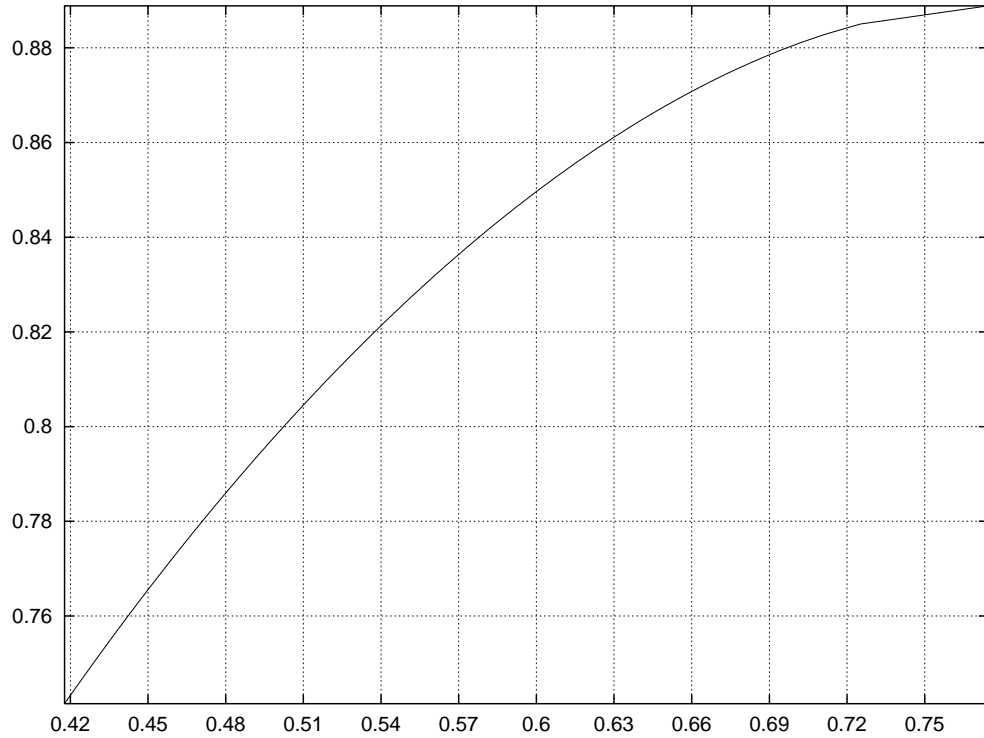


Fig. 6.— Normalized scaling exponent $\zeta(2)/\zeta(3)$ (vertical axis) as a function of the normalized scaling exponent $\zeta(1)/\zeta(3)$ (horizontal axis), as given by formula (2) with $\Theta = 1/3$ and $\Delta = 2/3$. The corresponding change of parameter D is in the interval $[2; 2\frac{1}{3}]$. The results of our numerical simulations correspond to $D = 2$, i.e. $\zeta(1)/\zeta(3) = 0.42$ and $\zeta(2)/\zeta(3) = 0.74$.